Available online at www.sciencedirect.com
ScienceDirect
Bioorganic & Medicinal Chemistry Letters 17 (2007) 5384–5389
Bioorganic & Medicinal Chemistry Letters

# Design and synthesis of quinolin-2(1*H*)-one derivatives as potent CDK5 inhibitors

Wenge Zhong,[a,*] Hu Liu,[a,†] Matthew R. Kaller,[a] Charles Henley,[b] Ella Magal,[b] Thomas Nguyen,[a] Timothy D. Osslund,[a] David Powers,[a] Robert M. Rzasa,[a] Hui-Ling Wang,[a] Weiya Wang,[b] Xiaoling Xiong,[a] Jiandong Zhang[a] and Mark H. Norman[a]

[a]*Chemistry Research and Discovery, Amgen Inc., One Amgen Center Drive, Thousand Oaks, CA 91320, USA*
[b]*Department of Neuroscience, Amgen Inc., One Amgen Center Drive, Thousand Oaks, CA 91320, USA*

Received 5 June 2007; revised 28 July 2007; accepted 30 July 2007
Available online 6 August 2007

**Abstract**—Cyclin-dependent kinase 5 (CDK5) is a serine/threonine protein kinase and its deregulation is implicated in a number of neurodegenerative disorders such as Alzheimer's disease, amyotrophic lateral sclerosis, and ischemic stroke. Using active site homology modeling between CDK5 and CDK2, we explored several different chemical series of potent CDK5 inhibitors. In this report, we describe the design, synthesis, and CDK5 inhibitory activities of quinolin-2(1*H*)-one derivatives.


Cyclin-dependent kinase 5 (CDK5) is a serine/threonine protein kinase believed to play a critical role in the early development of the central nervous system.[1,2] It has no known involvement in cell cycle progression, but it is shown to be involved in cellular processes such as neuronal differentiation,[3] cell adhesion,[4] and axonal guidance.[5] Recently, a large body of evidence suggests that deregulation of CDK5 is implicated in the pathology of a number of neurodegenerative disorders.[6–8] As a consequence, CDK5 inhibitors are of potential therapeutic uses for diseases such as Alzheimer's disease,[6] Parkinson's disease,[7] amyotrophic lateral sclerosis,[8] and ischemic stroke.[9] Several different classes of CDK5 inhibitors have recently appeared in the literature.[10]

From high throughput screening efforts, we identified a series of acyclic thiazolo-urea compounds as potent CDK2 and CDK5 inhibitors.[11,12] Based on the co-crystal structure of CDK2 and acyclic urea **1** (Fig. 1, CDK2 $IC_{50}$ = 4.6 nM; CDK5 $IC_{50}$ = 15 nM), we developed an active site homology model of CDK5 for further exploration and optimization of potent CDK5 inhibitors.[13] To mimic the intramolecular hydrogen bond between N1 and N3–H in urea **1**, which was believed to help pre-organize the inhibitor to a U-shaped binding conformation, we investigated ring-constrained CDK5 inhibitors (Fig. 1). We recently described a series of 3,4-dihydro-1*H*-quinazolin-2-ones that showed potent CDK5 inhibitory activities (**2**, CDK5 $IC_{50}$ = 79 nM).[13] To extend our investigations of ring-constrained systems, we examined the analogous quinolin-2(1*H*)-one derivatives. We proposed that quinolin-2(1*H*)-one derivatives such as **3** should overlay ideally with the core structures of the 3,4-dihydro-1*H*-quinazolin-2-ones and the same donor–acceptor hydrogen bond pattern for binding would project to the linker residues of the CDK5 active site. Herein we report the design, synthesis,

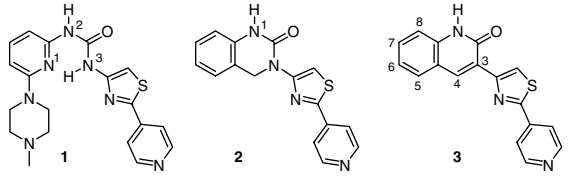

**Figure 1.** CDK5 inhibitors.

*Keywords*: Kinase; Neurodegenerative disorders; CDK5 inhibitor; Quinolin-2(1*H*)-one.
* Corresponding author. Tel.: +1 805 447 5732; fax: +1 805 480 3016; e-mail: zwenge@amgen.com
† Current address: Cambridge Laboratories, Pfizer Global R&D, 620 Memorial Drive, Cambridge, MA 02139, USA.

0960-894X/$ - see front matter © 2007 Elsevier Ltd. All rights reserved.
doi:10.1016/j.bmcl.2007.07.045

and CDK5 inhibitory activities of the quinolin-2(1*H*)-one derivatives.

A general synthesis of the quinolin-2(1*H*)-one derivatives is outlined in Scheme 1. Treatment of commercially available thioisonicotinamide **4** with chloroacetoacetate in refluxing MeOH provided methyl 2-(2-(pyridin-4-yl)thiazol-4-yl)acetate **5**.[14] Alkylation of **5** with appropriately substituted *o*-nitro benzylbromides **6** afforded intermediates **7**. Subsequent reductive cyclization of **7** with Fe/$NH_4Cl$ in refluxing aqueous EtOH furnished 3,4-dihydro-quinolin-2(1*H*)-ones **8** in good overall yield.[15] Treatment of **8** with NBS/AIBN in $CCl_4$ at 85 °C proceeded smoothly to provide quinolin-2(1*H*)-one derivatives **3**, **9a** and **b**, or **9d–f**.[16] For analogs **9c**, the synthesis was completed with ester hydrolysis using lithium hydroxide in aqueous MeOH and amide formation using standard EDCI–HOAt coupling conditions.

An alternative method for synthesizing derivatives bearing substituents at the 4-position of the quinolin-2(1*H*)-one core was employed. As shown in Scheme 2, compound **5** was hydrolyzed to provide the corresponding acid **10**, which was coupled to *o*-substituted anilines **11** using EDCI–HOAt to afford key intermediates **12**. Treatment of **12** with strong bases such as KO$^t$Bu or LiHMDS led to the formation of the 4-substituted quinolin-2(1*H*)-one derivatives **13a–g**.[17]

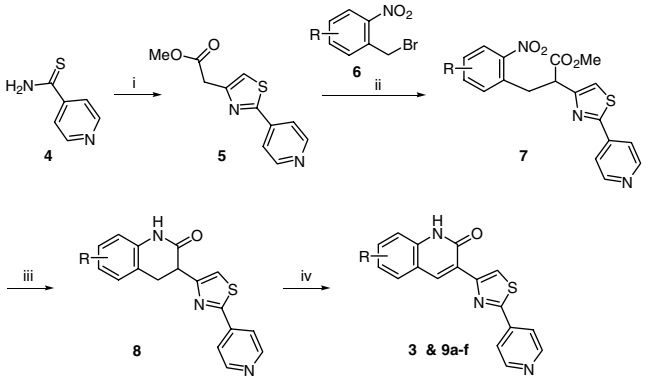


**Scheme 1.** Reagents and conditions: (i) $ClCH_2COCH_2CO_2CH_3$, MeOH, reflux, 12 h; (ii) LiHMDS, THF, −78 °C, 1.5 h; (iii) Fe, $NH_4Cl$, $H_2O$–EtOH (1:1), 80 °C, 2 h; (iv) NBS, AIBN, $CCl_4$, 85 °C, 2 h; for **9c**, additional steps were: (a) LiOH, MeOH, $H_2O$, 75 °C, 2 h; (b) EDCI, HOAt, $^i$Pr$_2$NEt, amine, $CH_2Cl_2$, 0 °C—room temperature, 12 h.

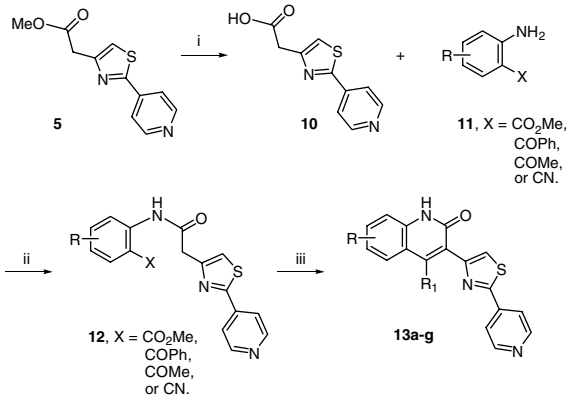


**Scheme 2.** Reagents and conditions: (i) LiOH, $H_2O$, MeOH, 75 °C, 2 h; (ii) EDCI, HOAt, $^i$Pr$_2$NEt, $CH_2Cl_2$, 0 °C—room temperature, 12 h; (iii) KO$^t$Bu or LiHMDS, THF, 0 °C—room temperature, 12 h.

To prepare a wide range of analogs that were intended to replace the pyrid-4-yl group of **3**, a flexible three-step parallel synthesis strategy based on thiazole ring formation was developed (Scheme 3). Using this method, readily available 2-aminobenzaldehydes **14** were reacted with diketene to provide 3-acetyl-quinolin-2(1*H*)-ones **15** in good yield.[18] Treatment of **15** with 5,5-dibromobarbituric acid (0.55 equiv) in refluxing THF afforded the versatile intermediate 3-bromoacetyl-quinolin-2(1*H*)-ones **16**, which precipitated out upon cooling of the reaction mixture.[19] In the final step, thiazole formation of **16** with a variety of thioamides in MeOH furnished quinolin-2(1*H*)-one derivatives **17a–p**.[14] In most cases the final products precipitated from the reaction mixtures and simple filtration was sufficient for obtaining final products with >95% purity. It should be noted that this chemistry was also applied to the synthesis of inhibitors **9g–i**, wherein two sequential steps of ester hydrolysis and amide formation were followed.

The derivatives prepared in this study were evaluated for their ability to inhibit purified human CDK5. Compounds were screened in an HTRF human CDK5/p25 assay that was run in the presence of 25 μM ATP and 1 μM histone-H1. The $IC_{50}$ values were determined from dose–response curves and are reported in Tables 1–4 as the average of two replications (unless otherwise indicated).

To validate the quinolin-2(1*H*)-one as a viable alternative core to the 3,4-dihydro-1*H*-quinazolin-2-one, we prepared compound **3** and found it to be a potent CDK5 inhibitor ($IC_{50}$ = 54 nM). With this encouraging result, we started our investigation by systematically introducing various modifications at the 5-, 6-, and 7-positions of the quinolin-2(1*H*)-one core. Table 1 highlights the findings. At the 5-position, an ester group was well tolerated (**9a**, $IC_{50}$ = 33 nM), but a carboxyl group was detrimental to activity (**9b**, $IC_{50}$ > 10 μM).

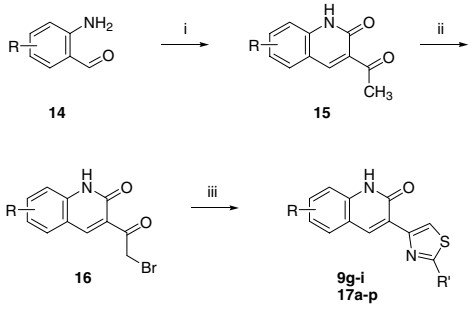


**Scheme 3.** Reagents and conditions: (i) diketene, DMAP, $CH_2Cl_2$, 50–80%; (ii) 5,5-dibromobarbituric acid (0.55 equiv), THF, reflux, 2–4 h, 70–80%; (iii) R′-CSNH$_2$, MeOH, 75 °C, 12 h; for **9g–i**, additional steps were: (a) NaOH, MeOH, $H_2O$, 75 °C, 2 h; (b) pivaloyl chloride, $^i$Pr$_2$NEt, amine, $CH_2Cl_2$, 0 °C—room temperature, 12 h.

**Table 1.** SAR of substituted 3-(2-pyridin-4-yl-thiazol-4-yl)quinolin-2(1*H*)-ones

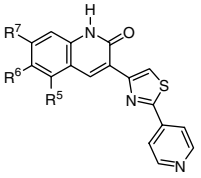

| Compound | $R^5$ | $R^6$ | $R^7$ | CDK5/p25 ($IC_{50}$; nM)[a] |
|---|---|---|---|---|
| **3** | H | H | H | 54 ± 33 |
| **9a** |  | H | H | 33 ± 25 |
| **9b** |  | H | H | >10,000 |
| **9c** |  | H | H | 480 ± 100 |
| **9d** | H | F | H | 110 ± 69 |
| **9e** | H | Cl | H | 11 ± 7.0 |
| **9f** | H | H | $CF_3$ | 6.3[b] |
| **9g** | H | H | 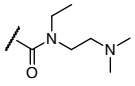 | 8.3[b] |
| **9h** | H | H | 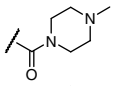 | 4.4 ± 0.7 |
| **9i** | H | H |  | 2.7[b] |

[a] At least two independent experiments were performed for each compound to determine the $IC_{50}$ values.
[b] One experiment was performed to determine the $IC_{50}$ value.

**Table 2.** SAR of substituted 3-(2-pyridin-4-yl-thiazol-4-yl)quinolin-2(1*H*)-ones

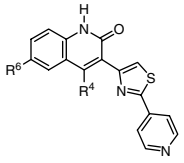

| Compound | $R^4$ | $R^6$ | CDK5/p25 ($IC_{50}$; nM)[a] |
|---|---|---|---|
| **3** | H | H | 54 ± 33 |
| **13a** | OH | H | 160 ± 98 |
| **13b** |  | H | 470 ± 220 |
| **13c** | $CH_3$ | H | 2800 ± 1500 |
| **13d** | $NH_2$ | H | 11 ± 7.0 |
| **13e** | $NH_2$ | Cl | 3.8[b] |
| **13f** | $NH_2$ |  | 250 ± 210 |
| **13g** | $NH_2$ |  | 120 ± 36 |

[a] At least two independent experiments were performed for each compound to determine the $IC_{50}$ values.
[b] One experiment was performed to determine the $IC_{50}$ value.

**Table 3.** SAR of pyridin-4-yl replaced thiazol-4-yl-quinolin-2(1*H*)-ones

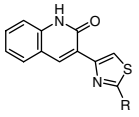

| Compound | R | CDK5/p25 ($IC_{50}$; nM)[a] |
|---|---|---|
| **3** |  | 54 ± 33 |
| **17a** |  | 1400 ± 81 |
| **17b** |  | 410 ± 190 |
| **17c** |  | 50 ± 26 |
| **17d** |  | >10,000[b] |
| **17e** | 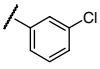 | >10,000[b] |
| **17f** | 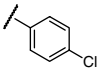 | >10,000[b] |
| **17g** | 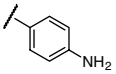 | 170 ± 77 nM |
| **17h** | 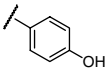 | 24 ± 15 |
| **17i** | 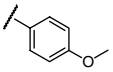 | >10,000[b] |

[a] At least two independent experiments were performed for each compound to determine the $IC_{50}$ values.
[b] One experiment was performed to determine the $IC_{50}$ value.

Tertiary amido groups were then incorporated at this position. It had been established earlier that such amido groups at the corresponding position in the acyclic urea series were beneficial for activities (data not shown). Surprisingly, we did not observe a similar SAR trend in the quinolin-2(1*H*)-one series. The best of these amido analogs, a diethylamido derivative **9c**, was only moderately active ($IC_{50}$ = 480 nM). While the 6-fluoro analog **9d** was slightly less active than compound **3**, the 6-chloro analog **9e** was about 5-fold more potent ($IC_{50}$ = 11 nM). As in the 3,4-dihydro-1*H*-quinazolin-2-one series, the 7-position was found to be the most permissive to modifications.[13] For example, introduction of a $CF_3$ group (**9f**) increased the potency by approximately 9-fold. In contrast to the SAR trend observed at the 5-position, a variety of analogs containing tertiary amido groups at this position were among the most potent CDK5 inhibitors in this series with $IC_{50}$ values ranging from 2.7 to 8.3 nM (**9g–i**). This was not very surprising since the CDK5 active site homology model suggested that the

**Table 4.** SAR of pyridin-4-yl replaced thiazol-4-yl-quinolin-2(1*H*)-one arylsulfone derivatives

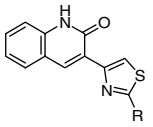

| Compound | R | CDK5/p25 ($IC_{50}$; nM)[a] |
|---|---|---|
| **3** |  | 54 ± 33 |
| **17j** | 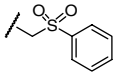 | 29 ± 19 |
| **17k** | 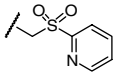 | 10 ± 1.1 |
| **17l** | 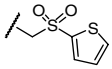 | 2.1 ± 1.1 |
| **17m** | 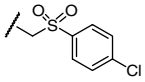 | 240 ± 150 |
| **17n** |  | 300 ± 160 |
| **17o** |  | 6900 ± 1000 |
| (±)-**17p** | 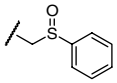 | 120 ± 47 |

[a] At least two independent experiments were performed for each compound to determine the $IC_{50}$ values.

7-position is close to a solvent exposed area from the active site and should be more tolerant to substitutions.

Table 2 summarizes the results from the 4-substituted quinolin-2(1*H*)-one derivatives. In comparison to compound **3**, substitution with a hydroxyl, phenyl, or methyl group at this position provided inhibitors **13a**, **13b**, and **13c** that were 3-, 9-, and 55-fold less active, respectively. However, an amino group at this position provided superior CDK5 activity. Compound **13d** was about 5-fold more potent than compound **3**. With the 4-amino group in place, additional substituents were amended at the 6-position. While small electron-withdrawing group such as chloro resulted in an additional 3-fold increase in potency over **13d**, large electron-donating groups such as 1-piperidinyl or 4-methyl-1-piperizinyl groups resulted in a 10- to 20-fold decrease in activity (**13e**–**g**).

In the 3,4-dihydro-1*H*-quinazolin-2-one series, we had shown that the pyrid-4-yl group was optimal for enzyme activity.[13] In the homology model, it was believed that the pyrid-4-yl group is engaged in a hydrogen bond network involving a salt bridge formed by two highly conserved residues Lys33 and Asp144. However, considering the potential Cyp P450 inhibitory liabilities frequently associated with pyridyl-containing compounds,[20] we investigated replacements for this group. Facilitated by a three-step parallel synthetic strategy, we were able to readily access the desired analogs.

Table 3 summarizes the CDK5 inhibitory activities of selected compounds with alternatives to the pyrid-4-yl group. Not surprisingly, replacement of the pyrid-4-yl group with a phenyl group resulted in a significant decrease of activity (**17a**, $IC_{50}$ = 1400 nM). This may be attributed to the loss of the ability to interact with the salt bridge formed between Lys33 and Asp144. Consistent with this observation, the thien-3-yl analog **17b** also exhibited an 8-fold decrease in activity. However, the pyrid-3-yl analog **17c** was equipotent as compound **3**, despite the less than optimal positioning of the 3-N atom for simultaneous interactions with both Lys33 and Asp144 in the homology model. We attempted to improve potency of **17a** by introducing substituents onto the phenyl ring. Substitution scanning with chloro at the 2-, 3-, or 4-position of the phenyl ring of **17a** provided inhibitors with additional loss of activity (**17d**–**f**, Table 3), suggesting unfavorable van der Waals interactions between this portion of the inhibitor and the active site of CDK5. However, a closer examination of the homology model revealed that the Lys33–Asp144 salt bridge was at the edge toward a solvent exposed area. We reasoned that certain hydrophilic substituents at the 4-position of the phenyl ring may be tolerated. Indeed, we found that introduction of an amino or a hydroxyl group at the 4-position afforded potent inhibitors **17g** and **17h**, with the latter being 2-fold more potent than compound **3**. The observed potency increases may be attributed to the favorable interactions of the amino or the hydroxy group with the Lys33–Asp144 salt bridge. The hydrogen donor abilities of these groups appeared to be important, as the 4-methoxy derivative **17i** was >400-fold less active than **17h**.

In order to probe different potential binding interactions at the CDK5 active site, we explored other structurally diverse pyrid-4-yl alternatives. We discovered an interesting series of quinolin-2(1*H*)-one arylsulfone derivatives as potent CDK5 inhibitors (Table 4). For example, arylsulfone derivatives **17j**, **17k**, and **17l** exhibited potencies of 29, 10, and 2.1 nM, respectively. The aryl ring was found to be sensitive to modifications as seen with the introduction of chloro at the 4-position of the phenyl ring of **17j** leading to >8-fold decrease in activity (**17m**, $IC_{50}$ = 240 nM). Attempts to replace the aryl rings with simple alkyl groups were unsuccessful. While the methylsulfone derivative **17n** retained moderate potency, the *tert*-butylsulfone analog **17o** was >240-fold less active. Finally, we determined that the sulfone moiety was important for activity. As shown in Table 3, the corresponding mono-sulfoxide analog of **17j** displayed an $IC_{50}$ of 1100 nM ((±)-**17p**).

To better understand the binding mode of the quinolin-2(1*H*)-one arylsulfone inhibitors, we chose **17j** as a representative example and modeled it in the CDK5 active site.[21] In the model illustrated in Figure 2, the inhibitor binds in a J-shaped conformation whereby the quinolin-2(1*H*)-one core forms two key hydrogen bonds to Cys83 in the linker. Consistent with the

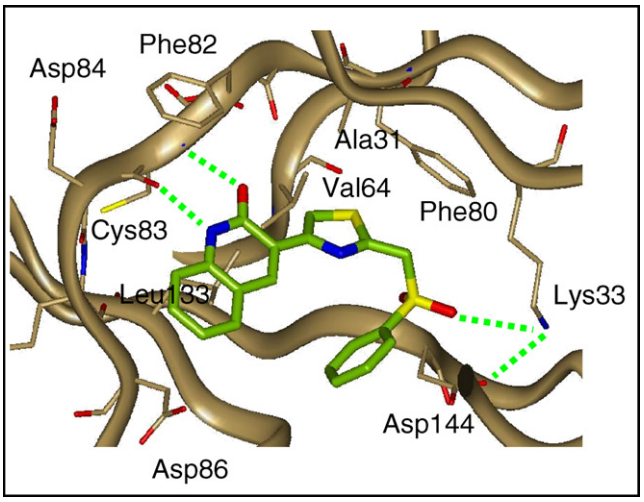


**Figure 2.** Binding model of compound **17j** in the active site of CDK5. Proposed H-bonding network is shown in green. Carbon atoms of compound **17j** are shown in green, carbon atoms of active site residues in brown, nitrogen atoms in blue, oxygen in red, and sulfur in yellow.

3,4-dihydro-1*H*-quinazolin-2-one series, and our original hypothesis, the thiazole ring extends into the conserved hydrophobic pocket lined in part by Phe80 and forms an edge-to-face van der Waals interaction with Phe80. The phenyl group of the arylsulfone moiety provides additional hydrophobic interactions. Interestingly, one of the oxygen atoms of the sulfone moiety interacts with the Lys33–Asp144 salt bridge by forming a hydrogen bond to the $\varepsilon$-$NH_2$ group of Lys33, while the other oxygen atom forms a potential hydrogen bond with the backbone NH of Asp144. This mode of interaction differs significantly from that of the pyrid-4-yl group in the co-crystal structure of CDK2 and inhibitor **1** and provides a rational basis to explain the observed SAR trends of these quinolin-2(1*H*)-one arylsulfone inhibitors.

To summarize, using active site homology modeling based on crystallographic data from the acyclic urea **1**/CDK2 complex, we rationally designed and synthesized a novel series of quinolin-2(1*H*)-one derivatives as potent CDK5 inhibitors. From these studies, we found that the 4-amino substituent at the quinolin-2(1*H*)-one core was well tolerated and the 7-position was the most permissive for modifications. In our effort to explore pyrid-4-yl alternatives, we discovered a series of arylsulfone compounds as potent CDK5 inhibitors. A binding model was developed for an exemplary compound from this class of compounds to account for the major binding interactions. Further investigations toward improving solubility and selectivity of the quinolin-2(1*H*)-one derivatives will be reported in due course.

## Acknowledgments

We are grateful to Dr. Vellarkad Viswanadhan for modeling support and Dr. Ning Xi for proofreading this manuscript and providing valuable suggestions.

## References and notes

1. Dhavan, R.; Tsai, L.-H. *Nat. Rev. Mol. Cell Biol.* **2001**, *2*, 749.
2. Smith, D. S.; Tsai, L.-H. *Trends Cell Biol.* **2003**, *12*(1), 28.
3. Nikolic, M.; Dudek, H.; Kwon, Y. T.; Ramos, Y. F.; Tsai, L. H. *Genes Dev.* **1996**, *10*, 816.
4. Kwon, Y. T.; Gupta, A.; Zhou, Y.; Mikolic, M.; Tsai, L. H. *Curr. Biol.* **2000**, *10*, 363.
5. Kwon, Y. T.; Tsai, L. H.; Crandell, J. E. *J. Comp. Neurol.* **1999**, *415*, 218.
6. (a) Tsai, L.-H.; Lee, M.-S.; Cruz, J. *Biochim. Biophys. Acta* **2004**, *1697*, 137; (b) Maccioni, R. B.; Otth, C.; Concha, I. I.; Munoz, J. P. *Eur. J. Biochem.* **2001**, *268*, 1518.
7. Smith, P. D.; Crocker, S. J.; Jackson-Lewis, V.; Jordan-Sciutto, K. L.; Hayley, S.; Mount, M. P.; O'Hare, M. J.; Callaaghan, S.; Slack, R. S.; Przedborski, S. *Proc. Natl. Acad. Sci* **2003**, *100*, 13650.
8. Patzke, H.; Tsai, L.-H. *Trends Neurosci.* **2002**, *25*, 8.
9. (a) Wang, J.; Lui, S.; Fu, Y.; Wang, J. H.; Lu, Y. *Nat. Neurosci.* **2003**, *6*, 1039; (b) Weishaupt, J. H.; Kussmaul, L.; Grotsch, P.; Heckel, A.; Rohde, G.; Romig, H.; Bahr, M.; Gillardson, F. *Mol. Cell. Neurosci.* **2003**, *24*, 489; (c) Wang, F.; Corbett, D.; Osuga, H. *J. Cereb. Blood Flow Metab.* **2002**, *22*, 171; (d) Osuga, H.; Osuga, S.; Wang, F.; Fetni, R.; Hogan, M. J.; Slack, R. S.; Hakim, A. M.; Ikeda, J. E.; Park, D. S. *Proc. Natl. Acad. Sci* **2000**, *97*, 10254.
10. (a) Gompel, M.; Leost, M.; Bal de Kier Joffe, E.; Puricelli, L.; Franco, L. H.; Palermo, J.; Meijer, L. *Bioorg. Med. Chem. Lett.* **2004**, *14*, 1703; (b) Polychronopoulos, P.; Magiatis, P.; Skaltsounis, A.-L.; Myrianthopoulos, V.; Mikros, E.; Tarricone, A.; Musacchio, A.; Roe, S. M.; Pearl, L.; Maryse, L.; Greengard, P.; Meijer, L. *J. Med. Chem.* **2004**, *47*, 935; (c) Zapata-Torres, G.; Opazo, F.; Salgado, C.; Munoz, J. P.; Krautwurst, H.; Mascayano, C.; Sepulveda-Boza, S.; Maccioni, R. B.; Cassels, B. K. *J. Nat. Prod.* **2004**, *67*, 416; (d) Ortega, M. A.; Montoya, M. E.; Zarranz, B.; Jaso, A.; Aldana, I.; Leclerc, S.; Meijer, L.; Monge, A. *Bioorg. Med. Chem.* **2002**, *10*, 2177; (e) Chang, Y. T.; Gray, N. S.; Rosania, G. R.; Sutherlin, D. P.; Kwon, S.; Norman, T. C.; Sarohia, R.; Leost, M.; Meijer, L.; Schultz, P. G. *Chem. Biol.* **1999**, *6*, 361; (f) Helal, C. J.; Sanner, M. A.; Cooper, C. B.; Gant, T.; Adam, M.; Luca, J. C.; Kang, Z.; Kupchinsky, S.; Ahlijanian, M. K.; Tate, B.; Menniti, F. S.; Kelly, K.; Peterson, M. *Bioorg. Med. Chem. Lett.* **2004**, *14*, 5521.
11. Santora, V.; Askew, B.; Ghose, A.; Hague, A.; Kim, T. S.; Laber, E.; Li, A.; Lian, B.; Liu, G.; Norman, M. H.; Smith, L.; Tasker, A.; Tegley, C.; Yang, K. International Patent WO 02/014311, 2002.
12. Hever, G.; Wang, J.; Kuang, R.; Zhang, M.; Jiao, S.; Louis, J. C.; Magal, E. CDK5 Inhibition as a Target for Neuroprotection in Rat Model of Middle Cerebral Artery Occlusion. Society for Neuroscience 33rd Annual Meeting, New Orleans, 2003.
13. Rzasa, R. M.; Kaller, M.; Liu, G.; Magal, E.; Nguyen, T.; Osslund, T. D.; Powers, D.; Santora, V. J.; Wang, H.-L.; Xiaoling Xiong, X.; Zhong, W.; Norman, M. H. *Bioorg. Med. Chem.* **2007**. doi:10.1016/j.bmc.2007.07.005.
14. El Kazzouli, S.; Berteina-Raboin, S.; Mouaddib, A.; Guillaumet, G. *Tetrahedron Lett.* **2002**, *43*, 3193.
15. Palacios, F.; Herrán, E.; Rubials, G. *J. Org. Chem.* **1999**, *64*, 6239.
16. Teramoto, S.; Tanaka, M.; Shimizu, H.; Fujioka, T.; Tabusa, F.; Imaizumi, T.; Yoshida, K.; Fujiki, H.; Mori, T.; Sumida, T.; Tominaga, M. *J. Med. Chem.* **2003**, *46*, 3033.

17. Rehwald, M.; Gewald, K.; Lankau, H.; Unverferth, K. *Heterocycles* **1997**, *45*, 483.
18. Davis, S. E.; Rauckman, B. S.; Chan, J. H.; Roth, B. *J. Med. Chem.* **1989**, *32*, 1936.
19. Burkhart, J. P.; Gates, C. A.; Laughlin, M. E.; Resvick, R. J.; Peet, N. P. *Bioorg. Med. Chem.* **1996**, *4*, 1411.
20. Fontana, E.; Dansette, P. M.; Poli, S. M. *Curr. Drug Metab.* **2005**, *6*, 413.
21. The arylsulfone analog **17k** was generated using Insight (2000) software with in-house X-ray structure of a related compound as the starting point. Ab initio calculations using Density Functional Theory as implemented in Gaussian98 software, utilizing the B3LYP hybrid density functional and the 6-31G* basis set at B3LYP/6-31G* level, were carried out on these molecules. These were aligned using Insight II, Transform/Superimpose options. Solvation free energies were calculated using the Polarizable Continuum Model (PCM) implemented in Gaussian 98 software.